Approximation of modal wavenumbers and group speeds in an oceanic waveguide using a neural network

Arthur Varon, Jerome I. Mars, Julien Bonnel

JASA Express Letters

JUNE 12 2023

Approximation of modal wavenumbers and group speeds in an oceanic waveguide using a neural network

A. Varon ; J. Mars ; J. Bonnel

JASA Express Lett. 3, 066003 (2023)
https://doi.org/10.1121/10.0019704

JASA EXPRESS LETTERS ARTICLE asa.scitation.org/journal/jel

Approximation of modal wavenumbers and group speeds in an oceanic waveguide using a neural network

A. Varon,[1,a] J. Mars,[1] and J. Bonnel[2]
[1]Université Grenoble Alpes, CNRS, Grenoble-INP, GIPSA-Lab, 38000 Grenoble, France
[2]Applied Ocean Physics and Engineering, Woods Hole Oceanographic Institution, Woods Hole, Massachusetts 02543, USA
arthur.varon@gipsa-lab.grenoble-inp.fr, jerome.mars@gipsa-lab.grenoble-inp.fr, jbonnel@whoi.edu

Abstract: Underwater acoustic propagation is influenced not only by the property of the water column, but also by the seabed property. Modeling this propagation using normal mode simulation can be computationally intensive, especially for wideband signals. To address this challenge, a Deep Neural Network is used to predict modal horizontal wavenumbers and group velocities. Predicted wavenumbers are then used to compute modal depth functions and transmission losses, reducing computational cost without significant loss in accuracy. This is illustrated on a simulated Shallow Water 2006 inversion scenario.

[Editor: Gopu R. Potty] https://doi.org/10.1121/10.0019704

Received: 28 March 2023 **Accepted:** 21 May 2023 **Published Online:** 12 June 2023

1. Introduction

Acoustic waves play a crucial role in underwater communication and sensing applications, as they can be used to detect objects, measure distances, and transmit information. However, the propagation of these waves in underwater environments is complex, as it is affected by the physical characteristics of the water column and the seabed. To describe the behavior of acoustic waves in shallow underwater environment, normal mode propagation models have been developed (Porter, 1992; Westwood *et al.*, 1996). Although normal mode codes are computationally tractable, running the simulation many times for inversion or broadband problems can be computationally expensive. This article explores the use of machine learning algorithms to accelerate the resolution of the normal mode forward propagation problem.

In the past decades, neural networks methods have gained significant attention thanks to their capacity to approximate non-linear functions (Hornik *et al.*, 1989). Their ability to simulate various physical phenomena (Adler *et al.*, 2021; Brunton *et al.*, 2020) while decreasing the computational costs of these simulations (Abdolrazzaghi *et al.*, 2018; Moseley *et al.*, 2020) has been well established.

The idea of using machine learning algorithms for underwater acoustic study is not new (Stéphan *et al.*, 1996). It has been used recently for various inverse problems including source localization (Durofchalk *et al.*, 2021; Goldwater *et al.*, 2021; Van Komen *et al.*, 2019) and seabed classification (Frederick *et al.*, 2020; Howarth *et al.*, 2022). However, it has barely been considered for forward physical simulations. One possible reason for this, may be the large variety of methods available to simulate the acoustic fields, as well as a lack of true labeled data to evaluate the trained models. Nevertheless, there have been some promising studies, such as those conducted by Mallik *et al.* (2022). In their work, they have trained a model to extend the prediction of transmission loss (TL) in range from several source/receiver locations. The model was trained on data generated using ray theory in a fixed environment (single Munk profile) for different source positions. The proposed model is able to extend the prediction of a given TL for untrained source position but requires large TL input sequences to be able to accurately generate the acoustic far field. Another noteworthy research is the work done by Li and Chitre (2022b), where they embedded the normal mode theory into a neural network to predict modal parameters from a measured acoustic field, and use it to predict the acoustic field outside of the measured region. They also proposed a higher frequency approach for the same type of application using ray theory (Li and Chitre, 2022a). In the present article, the approach is different. Our main objective is to replace normal mode physical codes by a faster (but approximated) neural network. We consider here a simple deep neural network (DNN), which is trained to predict modal horizontal wavenumbers and group speeds for various environmental inputs. The predicted wavenumbers can later be used to predict modal depth function, and thus TL, while the predicted group speed can be used to solve inverse problems.

[a]Author to whom correspondence should be addressed.

2. Underwater modal propagation

The underwater environment acts as a waveguide in which the acoustic field can be described using normal mode theory. In this framework, the pressure field in the frequency domain Y is described as a superposition of propagating modes m multiplied with the amplitude of a source signal S at the considered frequency f. The amplitude of a received mode is dependent on the modal depth function Ψ_m at the receiver and source depth, respectively noted z_r and z_s, as well as the range r between the source and the receiver and the horizontal modal wavenumber k_{rm}. Formally, the pressure field is given by

$$Y(f) = |S(f)| \sum_{m=1}^{N} \Psi_m(z_s,f)\Psi_m(z_r,f) \frac{e^{jrk_{rm}(f)}}{\sqrt{rk_{rm}(f)}}, \tag{1}$$

with N the number of propagating modes.

Further, the group velocity v_{gm} is given by

$$v_{gm}(f) = 2\pi \frac{\partial f}{\partial k_{rm}(f)}. \tag{2}$$

The dependence on frequency for the group velocities means that the underwater environment acts as a dispersive waveguide, where the dispersion depends on the properties of the waveguide. This makes using the dispersion suited for geoacoustic inversion, e.g., Bonnel *et al.* (2013) and Chapman and Shang (2021).

3. Method

The objective here is to replace the use of an underwater modal propagation simulation by a neural network to significantly reduce simulation time while still maintaining a high level of accuracy.

Let us assume here that an environment is described by a set of parameters θ (it may include geoacoustic and/or geometric parameters). Traditional normal mode codes take θ as an input and computes the associated wavenumbers k_{rm} and modal depth functions Ψ_m, which can be combined to evaluate TL. Group velocities v_{gm}, which are useful for inversion, can also be obtained from normal mode codes. Here, we train a neural network to predict k_{rm} and v_{gm} from θ. Modal depth functions Ψ_m are later obtained from θ and the predicted k_{rm} using the usual inverse iteration method (Jensen *et al.*, 2011), and TL can then be obtained by combining the predicted k_{rm} and associated Ψ_m following Eq. (1). This method is summarized in Fig. 1.

To train the neural network, a labeled dataset with various θ (neural network input) and associated k_{rm} and v_{gm} (neural network output) is required. It can be created with any traditional normal mode code. In this paper, KRAKEN will be used (Porter, 1992).

3.1 Data

The present letter focuses on a specific environment parameterization. The water column is modeled with a fixed sound speed profile (SSP). The seabed is modeled as a fluid with a single iso-speed iso-density sediment layer over an iso-speed iso-density basement, with geoacoustic parameters: sediment thickness h_1, sound speed c_1, density ρ_1, basement sound speed c_2, and density ρ_2. The frequency band of interest is kept fixed.

Once the environment parameterization is set, it is required to define parameter values (for fixed parameters, e.g., water SSP) or parameter boundaries (for varying parameters h_1, c_1, ρ_1, c_2, and ρ_2) to create datasets to train, validate and test the neural network. To mimic a realistic scenario, the water SSP is arbitrarily based on conditions encountered during SW06 shallow water experiment (Turgut, 2007). The water SSP is described using four nodes at depths 0, 10, 25, and 80 m with respective sound speed of 1525, 1525, 1485, and 1490 m/s. The density is constant through the water column and is equal to 1.03 kg/m^3. On the other hand, the five seafloor parameters h_1, c_1, ρ_1, c_2, and ρ_2 are variable. They can take value within wide bounds, as defined in Table 1.

To generate the training dataset, environments were randomly generated. To do so, the five seabed parameters were varied following a uniform distribution, using the bounds defined in Table 1. On the other hand, to generate the validation and test datasets, environments were deterministically generated using a 5D uniform grid. Such a grid is defined using 20 linearly spaced values for each of the seabed parameters, with bounds given by Table 1. This grid is then separated into two distinct intertwined sub-grids (with ten linearly spaced values for each seabed parameter): one of the sub-grid is used for the validation dataset and the other is used for the test dataset. This process ensures that training, validation and test datasets are distinct.

The simulation model (KRAKEN) is used on all these environments to obtain the wavenumbers and group velocities for frequencies from 150 to 300 Hz with 5 Hz increment for the first five propagating modes. Because the normal mode program used is unable to converge if the basement speed is not the maximum speed of the considered environment this results in a total of 50 000 distinct environment in both the validation and test dataset.

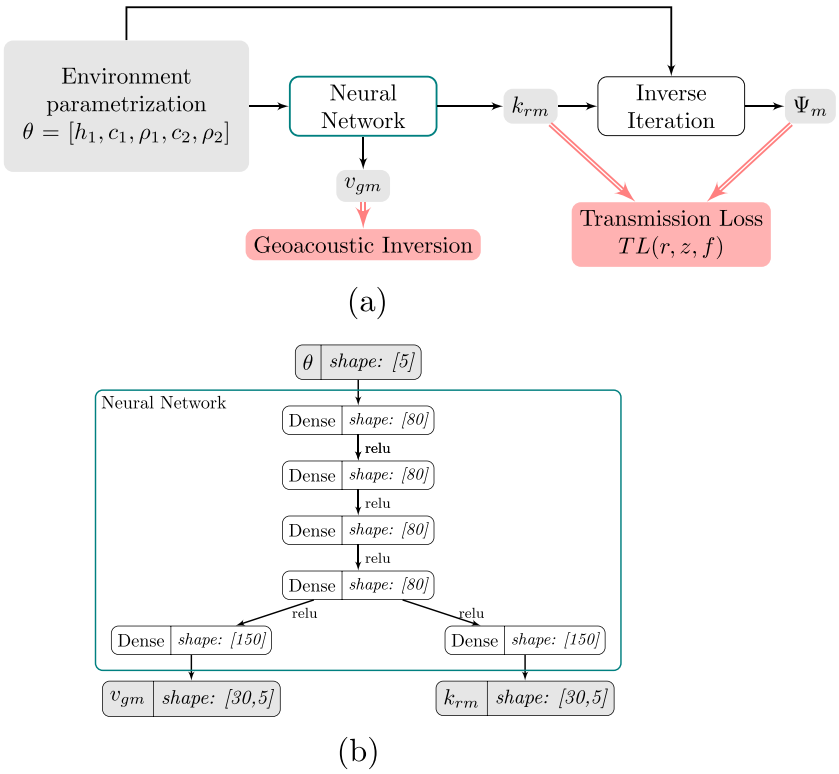

Fig. 1. (a) Data flow graph of the method. (b) Architecture of the neural network. For each operation, the indicated shape corresponds to the size of the output.

In order to improve the training of the model, the inputs (h_1, c_1, ρ_1, c_2, and ρ_2) are scaled between 0 and 1. The output group velocity v_{gm} is scaled using the same transformation as the input sound speeds (c_1 and c_2). Moreover, the linear tendency $2\pi f/c_{\text{water}}$ is subtracted from the wavenumber $k_{rm}(f)$ to focus the learning of the model on the dispersive behavior of the wavenumber. Here, c_{water} denote the weighted average of the sound speed in the water column. This preprocessing is comparable to a velocity correction often used in geosciences (Yilmaz, 2001).

3.2 Model description and training

The neural network used here is a simple DNN inspired by the work of Hansen and Cordua (2017) composed of four densely connected layers of 80 units each with rectified linear units plus a last densely connected layer outputting the predicted wavenumber and group velocity for every considered modes and frequencies. The details of the network is presented in Fig. 1(b).

The Adam optimizer (Kingma and Ba, 2014) is used for training with a learning rate of $\alpha = 10^{-2}$. The root mean squared error is used as a loss function to compare the predicted wavenumber k_{rm}^{pred} and group velocity v_{gm}^{pred} to the simulated ones $k_{rm}^{\text{truth}}, v_{gm}^{\text{truth}}$. To avoid overfitting issues, the learning rate was divided by two if the model did not improve on the validation data after two consecutive epochs, and the training was stopped if it did not improve after four consecutive epochs. After testing multiple sizes for the training dataset, it was found that a size of 400 000 was optimal. Table 2 provides network performance as a function of the size of the training dataset. Note that better performances are obtained

Table 1. Bounds for the environment parameters used to generate the training, validation, and test datasets.

Parameters	Units	Bound
Sediment thickness: h_1	m	[1,25]
Sediment sound speed: c_1	m/s	[1500, 2500]
Sediment density: ρ_1	kg/m^3	[1.2,2.5]
Basement sound speed: c_2	m/s	[1500, 2500]
Basement density: ρ_2	kg/m^3	[1.2,2.5]

Table 2. Prediction performance (RMSE) for various sizes of training datasets.

Size of the training dataset	k_{rm} (rad/m)	v_{gm} (m/s)
100 000	4.70×10^{-4}	2.27
200 000	2.30×10^{-4}	1.42
300 000	2.13×10^{-4}	1.06
400 000	1.51×10^{-4}	0.97
500 000	1.46×10^{-4}	0.93

with 500 000 training data values than 400 000 but the gain has been deemed insignificant. In the following, a training size of 400 000 is used.

3.3 Results

Once trained, the model can efficiently predict the wavenumbers and group velocities for the considered modes and frequencies. This is illustrated for a single environment in Figs. 2(a) and 2(d).

The overall performance is presented in Figs. 2(c) and 2(f), showing that the model is able to generalize in the test dataset, as the mean relative error between the truth and prediction per environment is less than 2.5% with the majority of environments below 0.5% of mean relative error. However, as can be shown in Fig. 2(b), the error on the predicted group velocity of the last considered propagating mode has the maximum amount of error and this is especially marked for lower frequency. This can be explained by the considered dataset, for which, the lower bound of the considered frequency is slightly below the cutoff frequency of the fifth mode. For these environments, there is high non-linearity as well as an inflection point which impacts the learning of the network. The same pattern can be observed in Fig. 2(e) for the error on the predicted wavenumber and this is also what explains the outlier in the distribution of mean relative error in Figs. 2(c) and 2(f).

4. Applications

Once the model is trained, it can be efficiently used for various normal mode-based applications. Two applications, TL computation and geoacoustic inversion, are presented in the following. Results of the proposed model will be compared to results obtained with a traditional normal mode propagation code (KRAKEN).

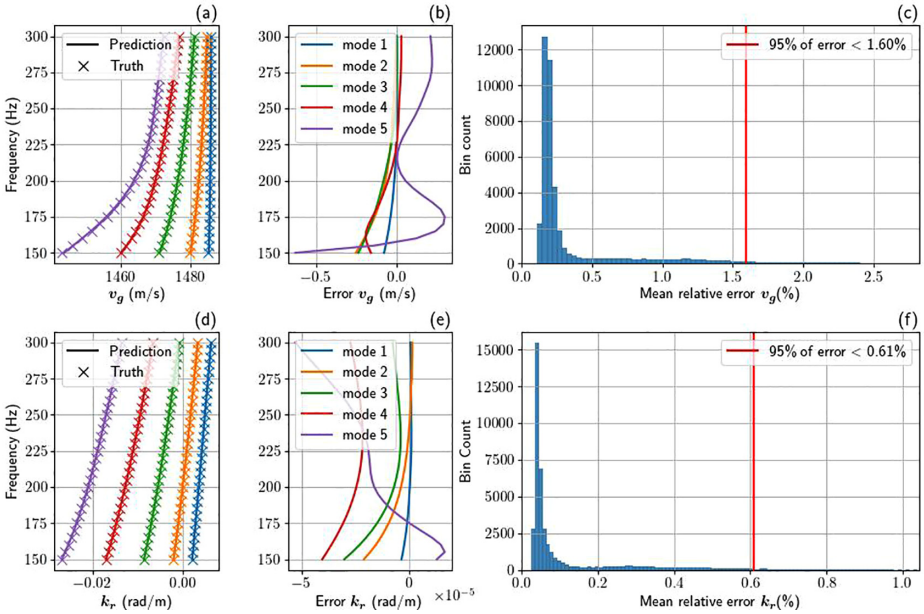

Fig. 2. Comparison of the dispersion in (a) the group velocity and (d) the wavenumber between the first five modes predicted by the DNN (prediction) and the output of the simulation using KRAKEN (truth). Error between the prediction and the simulation for (b) the group velocity and (e) the wavenumber. Overall performance in the test dataset for (c) the group velocity, (f) for the wavenumber. Panels (a), (b), (d), (e) are obtained for a single environment ($h_1 = 20.9$ m, $c_1 = 2111$ m/s, $\rho_1 = 2.29$ kg/m^3, $c_2 = 2180$ m/s, $\rho_2 = 2.30$ kg/m^3) while panel (c) and (f) are obtained on the whole test dataset.

4.1 Transmission loss

One proposed application of the trained model is TL computation. This is done by computing the modulus of the acoustic field, as given by Eq. (1). Since the trained model only provides the wavenumbers, it is first required to estimate the modal depth functions. As in most traditional normal mode codes, this is done using the inverse iteration method, as defined in Jensen *et al.* (2011). Examples of modal depth functions, obtained from wavenumbers predicted by our network, are shown in Fig. 3(a), and the associated errors between predictions (i.e., from our neural network) and truth (i.e., from KRAKEN) is shown in Fig. 3(b). This example illustrates the good capacity of the network to predict modal depth functions, with maximum errors two orders of magnitude below the maximum value. This result is representative of the performance obtained on other environments, which is not shown here for the sake of brevity.

The calculated modal depth functions are then combined with predicted wavenumbers to obtain the TL for set ranges and depths. An example of TL obtained using our method is shown in Fig. 3(d), while the truth (as obtained with KRAKEN) is shown in Fig. 3(c). Qualitatively, the two figures look fully similar. To quantify this, the absolute difference between prediction [Fig. 3(d)] and truth [Fig. 3(c)] is shown in Fig. 3(e). All the significant errors (>3 dB) are concentrated at locations where the TL are really high. This illustrates that the shape of the interference pattern is correctly predicted, but the TL values at the location of those inferences may be over/underestimated. The TL prediction performance is quantified on the test dataset through the root mean squared error between predicted and true TL for all the considered frequency and modes. A histogram of this error is shown in Fig. 3(f). It demonstrates a high level of accuracy with 99.5% of errors falling below 3 dB, and 80.4% of the root mean squared errors being lower than 1 dB.

4.2 Geoacoustic inversion

Another proposed application is the acceleration of computation speed for geoacoustic inversion. In these applications, a normal mode forward model is repeatedly called for many different environments to create a set of replicas. Geoacoustic parameters are then inferred from the simulated environment by matching replicas and measurements (Chapman and Shang, 2021). Many inversion methods exist, we focus here on those based on time-frequency modal dispersion (Ballard *et al.*, 2014; Bonnel *et al.*, 2020; Potty *et al.*, 2000), a quantity which is intrinsically related to the modal group speed v_{gm}.

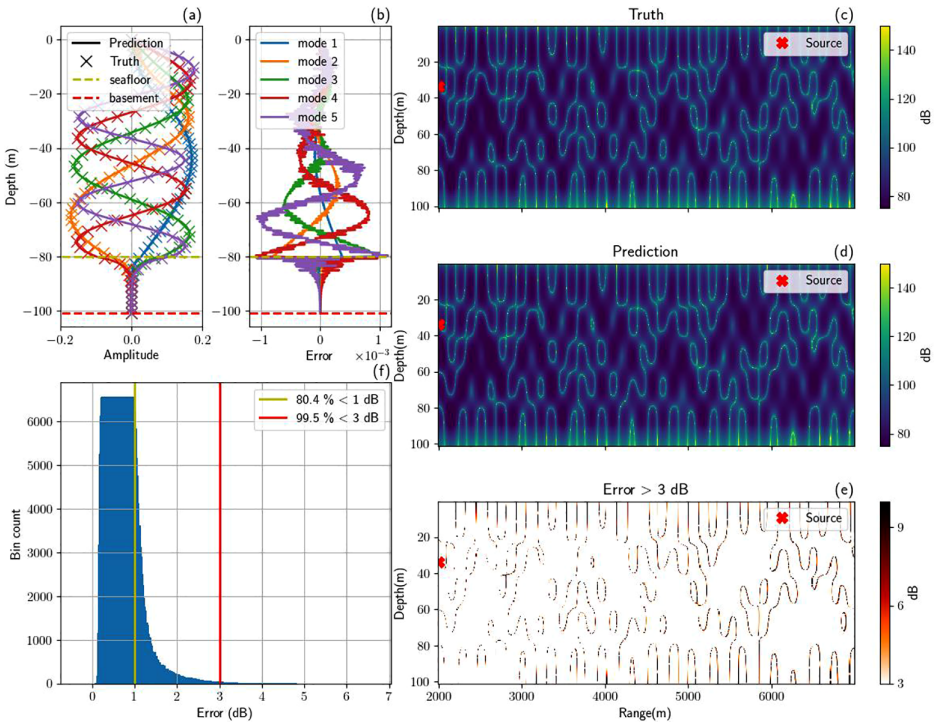

Fig. 3. (a) Comparison between the first five modal depths functions calculated at 150 Hz using the wavenumber predicted by the DNN (prediction) and the output of the simulation using KRAKEN (truth). (b) Error between the prediction (DNN) and the truth (KRAKEN) for each mode. Transmission loss calculation using the first five modes and frequency from 150 Hz to 300 Hz (c) using KRAKEN and (d) from DNN. (e) Absolute difference between the predicted TL from panel (d) and the truth TL from panel (c). (f) Histogram of the root mean squared error of the TL per environment for the whole test dataset. Panels (a)–(e) are obtained for a single environment ($h_1 = 20.9$ m, $c_1 = 2111$ m/s, $\rho_1 = 2.29$ kg/m^3, $c_2 = 2180$ m/s, $\rho_2 = 2.30$ kg/m^3).

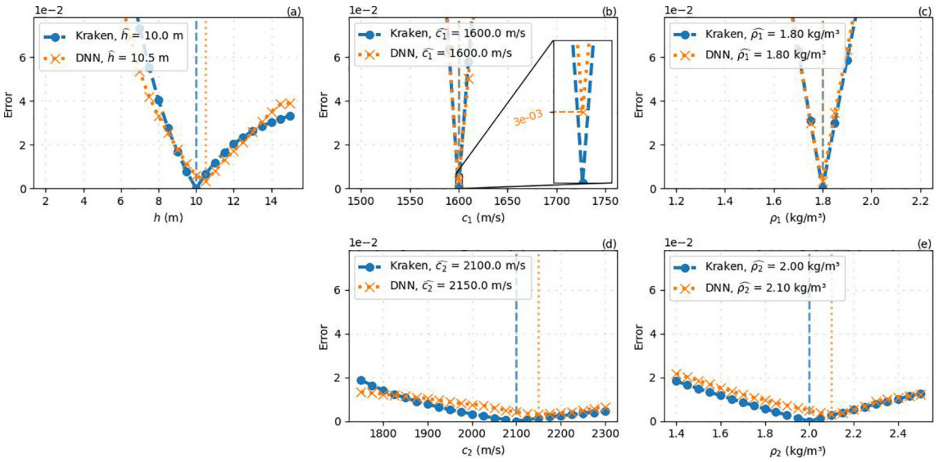

Fig. 4. Comparison of the root mean squared error on v_{gm} predicted by DNN and KRAKEN for the five variable environment parameters (h_1: thickness; c_1: sediment sound speed, ρ_1: sediment density, c_2: basement sound speed, ρ_2: basement density. The other variable parameters are fixed to get the minimum of error.

First, a set of reference modal group speed v_g^{truth} was calculated for the first four modes and 31 linearly spaced frequencies going from 150 to 300 Hz, using an environment based on the SW06 experiment (Turgut, 2007). This was done using the model described above with $h_1 = 10\,\text{m}$, $c_1 = 1600\,\text{m/s}$, $\rho_1 = 1.8\,\text{kg/m}^3$, $c_2 = 2100\,\text{m/s}$, $\rho_2 = 2.0\,\text{kg/m}^3$. Then, replicas were computed using both our model and KRAKEN. They are, respectively, noted v_{gm}^{DNN} and v_{gm}^{Krak}. To mimic inversion, the resulting group speeds are compared to the reference v_{gm}^{truth} using a simple root mean squared error

$$RMSE_i(\theta) = \sqrt{\frac{1}{N}\sum_{m,f}(v_{gm}^{\text{truth}^2} - v_{gm}^{i}(\theta)^2)}, \tag{3}$$

where i can express DNN or KRAKEN. The vector $\theta = [h_1, c_1, \rho_1, c_2, \rho_2]$ is swept over a five-dimensional grid within the boundaries defined in Table 1 and fine steps (0.5 m for h_1, 10 m/s for c_1, 0.05 kg/m^3 for ρ_1, 25 m/s for c_2, and 0.05 kg/m^3 for ρ_2), leading to about 7.5 million environments. Inversion results, both for the neural network (DNN) and for KRAKEN are presented in Fig. 4. On this figure, each panel is a slice of the 5D RMSE along one parameter, with all the other parameters taken at their optimal values (i.e., where the RMSE is minimal). As expected, since no noise was added on the data, inversion with KRAKEN is perfect: all the parameters are properly estimated with RMSE = 0. The results are slightly different for our DNN. All the sediment parameters (h_1, c_1, c_2) are perfectly estimated with the DNN, with a significantly small (but non-zero) RMSE. On the other hand, the basement parameters are estimated with a small error. This error (50 m/s for c_2 and 0.1 kg/m^3 for ρ_2) stays limited, particularly when compared to the poor sensitivity of the group speed to those parameters (as seen, for example, by the relative flatness of the associated RMSE curves). This further demonstrates the results of Fig. 4, and the good capacity of the network to predict modal dispersion.

Interestingly, using a similar implementation, simulating the 7.5×10^6 replicas took about 25 h using KRAKEN, and about 40 min with our trained DNN, which represents a 35-fold gain in computation speed. Note that such a gain is obtained after the DNN is trained, and that generating the 400 000 replica to train the DNN (see Sec. 3.1) required about 7.5 h.

5. Conclusion

The use of physics simulation in modal acoustics propagation can be excessively expensive, especially when repeated evaluations are required, such as in wideband signal propagation or for inversions method. As an alternative, using a machine learning model that reduces the computational time during inference was suggested. Although straightforward, the proposed model demonstrates remarkable accuracy, and obtained results are promising. After training, the neural network is able to predict modes (and TL) with a small error, while significantly reducing the computation time when compared to a traditional normal mode propagation code.

Here, the main limitation is that the question of generalization has not been tackled: the method has been developed with the assumption that the training conditions are representative of the application of interest. In practice, it is assumed that the water sound speed profile is perfectly known. Further, the considered frequency band has to be limited enough for the number of modes to be constant. When those conditions are met, the proposed method allows the prediction of modal propagation with limited computation complexity. A direct application for the method is to perform geoacoustic inversion in an area of interest using several experimental datasets collected during a short time period, provided that the water column sound speed profile can be assumed to be constant at the considered time and spatial scales.

In such a case, the neural network can be trained once and used several times to perform inversion on all the experimental datasets. This would drastically reduce the computational time required to obtain all the inversion results.

Acknowledgments

This research was supported by the French National Center for Scientific Research (CNRS), the French Defense Innovation Agency (AID) through the study and research convention 2021 65 003, and the U.S. Office of Naval Research (ONR).

References and links

Abdolrazzaghi, M., Hashemy, S., and Abdolali, A. (**2018**). "Fast-forward solver for inhomogeneous media using machine learning methods: Artificial neural network, support vector machine and fuzzy logic," Neural Comput. Appl. **29**(12), 1583–1591.

Adler, A., Araya-Polo, M., and Poggio, T. (**2021**). "Deep learning for seismic inverse problems: Toward the acceleration of geophysical analysis workflows," IEEE Signal Process. Mag. **38**(2), 89–119.

Ballard, M. S., Frisk, G. V., and Becker, K. M. (**2014**). "Estimates of the temporal and spatial variability of ocean sound speed on the new jersey shelf," J. Acoust. Soc. Am. **135**(6), 3316–3326.

Bonnel, J., Dosso, S. E., and Chapman, N. R. (**2013**). "Bayesian geoacoustic inversion of single hydrophone light bulb data using warping dispersion analysis," J. Acoust. Soc. Am. **134**(1), 120–130.

Bonnel, J., Thode, A., Wright, D., and Chapman, R. (**2020**). "Nonlinear time-warping made simple: A step-by-step tutorial on underwater acoustic modal separation with a single hydrophone," J. Acoust. Soc. Am. **147**(3), 1897–1926.

Brunton, S. L., Noack, B. R., and Koumoutsakos, P. (**2020**). "Machine learning for fluid mechanics," Annu. Rev. Fluid Mech. **52**(1), 477–508.

Chapman, N. R., and Shang, E. C. (**2021**). "Review of geoacoustic inversion in underwater acoustics," J. Theor. Comput. Acoust. **29**(03), 2130004.

Durofchalk, N. C., Jin, J., Vazquez, H. J., Gemba, K. L., Romberg, J., and Sabra, K. G. (**2021**). "Data driven source localization using a library of nearby shipping sources of opportunity," JASA Express Lett. **1**(12), 124802.

Frederick, C., Villar, S., and Michalopoulou, Z.-H. (**2020**). "Seabed classification using physics-based modeling and machine learning," J. Acoust. Soc. Am. **148**(2), 859–872.

Goldwater, M., Bonnel, J., Cammareri, A., Wright, D., and Zitterbart, D. P. (**2021**). "Classification of dispersive gunshot calls using a convolutional neural network," JASA Express Lett. **1**(10), 106002.

Hansen, T. M., and Cordua, K. S. (**2017**). "Efficient Monte Carlo sampling of inverse problems using a neural network-based forward—applied to GPR crosshole traveltime inversion," Geophys. J. Int. **211**(3), 1524–1533.

Hornik, K., Stinchcombe, M., and White, H. (**1989**). "Multilayer feedforward networks are universal approximators," Neural Netw. **2**(5), 359–366.

Howarth, K., Neilsen, T. B., Van Komen, D. F., and Knobles, D. P. (**2022**). "Seabed classification using a convolutional neural network on explosive sounds," IEEE J. Oceanic Eng. **47**(3), 670–679.

Jensen, F. B., Kuperman, W. A., Porter, M. B., and Schmidt, H. (**2011**). "Wavenumber integration techniques," in *Computational Ocean Acoustics* (Springer, New York), Chap. 4, pp. 233–335.

Kingma, D. P., and Ba, J. (**2014**). "Adam: A method for stochastic optimization," arXiv:1412.6980.

Li, K., and Chitre, M. (**2022a**). "Data-aided underwater acoustic ray propagation modeling," arXiv:2205.06066.

Li, K., and Chitre, M. (**2022b**). "Physics-aided data-driven modal ocean acoustic propagation modeling," in *The 24th International Congress on Acoustics* (*ICA*, *2022*).

Mallik, W., Jaiman, R. K., and Jelovica, J. (**2022**). "Predicting transmission loss in underwater acoustics using convolutional recurrent autoencoder network," J. Acoust. Soc. Am. **152**(3), 1627–1638.

Moseley, B., Nissen-meyer, T., and Markham, A. (**2020**). "Deep learning for fast simulation of seismic waves in complex media," Solid Earth **11**(4), 1527–1549.

Porter, M. B. (**1992**). "The Kraken normal mode program," technical report.

Potty, G. R., Miller, J. H., Lynch, J. F., and Smith, K. B. (**2000**). "Tomographic inversion for sediment parameters in shallow water," J. Acoust. Soc. Am. **108**(3), 973–986.

Stéphan, Y., Thiria, S., and Badran, F. (**1996**). "Application of multilayered neural networks to ocean acoustic tomography inversions," Inv. Problems Eng. **3**(4), 281–304.

Turgut, A. (**2007**). "Validation of high-resolution inversion techniques for measuring seabed geoacoustic properties during the onr-sw06 experiment," technical report.

Van Komen, D. F., Neilsen, T. B., Howarth, K., Knobles, D. P., and Dahl, P. H. (**2019**). "A convolutional neural network for source range and ocean seabed classification using pressure time-series," Proc. Mtgs. Acoust. **36**, 070004.

Westwood, E. K., Tindle, C. T., and Chapman, N. R. (**1996**). "A normal mode model for acousto–elastic ocean environments," J. Acoust. Soc. Am. **100**(6), 3631–3645.

Yilmaz, Ö. (**2001**). *Seismic Data Analysis: Processing, Inversion, and Interpretation of Seismic Data* (Society of Exploration Geophysicists, Houston), Chap. 3, pp. 274–288.